Thermodynamic Characterization of the Binding of Nucleotides to Glycyl-tRNA Synthetase†

John David Dignam,*,‡ Shadia Nada,‡ and Jonathan B. Chaires§

Department of Biochemistry and Molecular Biology, Medical College of Ohio, 3035 Arlington Avenue, Toledo, Ohio 43614-5804, and Department of Biochemistry, University of Mississippi Medical Center, 2500 North State Street, Jackson, Mississippi 39216-4505

Received February 4, 2003; Revised Manuscript Received March 19, 2003

ABSTRACT: The interaction of adenine nucleotides with glycyl-tRNA synthetase was examined by several experimental approaches. ATP and nonsubstrate ATP analogues render glycyl-tRNA synthetase more resistant to digestion by a number of proteases (thrombin, Arg-C, and chymotrypsin) at concentrations that correlate with their Michaelis constants or inhibition constants, consistent with their exerting an effect by binding at the ATP site. Glycine had little effect alone but potentiated the effect of ATP in increasing the resistance to thrombin digestion, consistent with the formation of an enzyme-bound adenylate. No protection from thrombin digestion was afforded by $tRNA^{gly}$. Binding constants were determined by isothermal titration calorimetry at 25 °C for ATP (2.5×10^5 M^{-1}), AMPPNP (3.7×10^5 M^{-1}), and AMPPCP (2.2×10^6 M^{-1}). The nucleotides had similar values for ΔH (−71 kJ mol^{-1}), with values for $T\Delta S$ that accounted for the differences in the binding constants. Near-ultraviolet CD spectra of the enzyme−nucleotide complexes indicate that the nucleotides are bound in the anti configuration. A glycyl-adenylate analogue, glycine sulfamoyl adenosine (GSAd), bound with a large value for ΔH (−187 kJ mol^{-1}), which was balanced by a large $T\Delta S$ term to give a binding constant (3.7×10^6 M^{-1}) only slightly larger than that of AMPPCP. Glycine binding to the enzyme could not be detected calorimetrically, and its presence did not change the thermodynamic parameters for binding of AMPPCP. AMPPNP and AMPPCP were not substrates for glycyl-tRNA synthetase. Analysis of the temperature dependence of ATP binding indicated that the heat capacity change is small, whereas the binding of GSAd is accompanied by a large negative heat capacity change (−2.6 kJ K^{-1} mol^{-1}). Titrations performed in buffers with different ionization enthalpies indicate that the large value for ΔH for the adenylate analogue does not arise from a coupled protonation event. Differential scanning calorimetry indicated that glycyl-tRNA synthetase is stabilized by nucleotides. Unfolding of the protein is irreversible, and thermodynamic parameters for unfolding could therefore not be determined. The results are consistent with a significant conformational transition in glycyl-tRNA synthetase coupled to the binding of GSAd.

Aminoacyl-tRNA synthetases catalyze reactions that result in the aminoacylation of tRNA (*1*−*3*). The fidelity of protein synthesis depends in part on the inherent specificity of these enzymes in the recognition of ligands and in some cases on editing activities (*4*−*7*) that remove misactivated amino acids and misacylated tRNAs. Although their direct role in protein synthesis was apparent from the time of their discovery (*8*−*10*), other unanticipated functions have been identified, including the role of mitochondrial leucyl- and tyrosyl-tRNA synthetases in the processing of group I introns (*11*−*13*), the apparent role of some enzymes as precursors to cytokines (*14*, *15*), and a recently identified function of tyrosyl-tRNA synthetase in angiogenesis (*16*, *17*).

At present there are structures, determined by X-ray crystallography, of examples of most of the eubacterial enzymes (*18*, *19*) and a limited number of proteins from eukaryotes (*20*−*23*). Differences in the structures of the unligated enzymes and complexes with ligands indicate that a few of these enzymes undergo significant conformational changes when they bind substrates. The amino acid binding sites of histidyl-tRNA (*24*), prolyl-tRNA (*25*), and tryptophanyl-tRNA (*26*) synthetases are formed as a result of structural rearrangements consistent with a classic induced fit model proposed by Koshland (*27*). Others, exemplified by *Thermus thermophilus* glycyl-tRNA synthetase (*28*), have an essentially preformed amino acid binding site; there are relatively minor differences between the amino acid, ATP, ethanolamine-ATP, and glycyl-adenylate ligated forms and the unligated form of the protein, more in keeping with the lock and key concept (*29*). Although the crystal structures contain a wealth of information with respect to how specific residues stabilize bound ligands in these complexes, proteins are not static and some conformational species may not be represented in the different crystalline forms. The inherent dynamic nature of transiently formed species would likely preclude their crystallization.

† This research was supported by a grant from the Medical College of Ohio Cancer Center (to J.D.D.) and Grant CA35635 from the National Cancer Institute, NIH (to J.B.C.).

* Corresponding author [telephone (419) 383-4136; fax (419) 383-6228; e-mail jdignam@mco.edu].

‡ Medical College of Ohio.

§ University of Mississippi Medical Center.

10.1021/bi030031h CCC: $25.00
Published on Web 04/18/2003

Glycyl-tRNA synthetases (*30*) from *T. thermophilus* (*28*, *31*), *Saccharomyces cerevisiae* (*32*), human (*33*−*35*), and *Bombyx mori* (*36*, *37*) are related, dimeric enzymes with the structural motifs characteristic of class II aminoacyl-tRNA synthetases (*38*). On the basis of sequence alignment, these enzymes likely have common structural elements but differ with respect to inserted and appended domains in the eukaryotic and archaeal proteins (*38*, *39*). That key residues in the *T. thermophilus* enzyme involved in binding substrates are conserved (*28*, *31*, *38*) suggests that the same types of contacts will stabilize binding of ligands in the eukaryotic enzymes. An N-terminal element in the human and insect enzymes, which is absent in the *T. thermophilus* enzyme, mediates binding to polynucleotides (*41*−*44*); this structural element appears in several eukaryotic aminoacyl-tRNA synthetases (*41*, *43*−*45*), and structures determined by NMR show that it forms an antiparallel coiled coil (*40*, *41*). Although there are some clues as to the function of the N-terminal element (*43*), the function of the inserted domains is unclear. These additional features of the eukaryotic enzymes may reflect functions not present in the bacterial enzyme and might result in significantly different ligand binding properties compared to the *T. thermophilus* protein.

To characterize the eukaryotic glycyl-tRNA synthetase, we examined the binding of nucleotide ligands including ATP, nonsubstrate ATP analogues, and an aminoacyl-adenylate analogue, glycine sulfamoyl adenosine (GSAd),[1] using protection from proteolysis, titration calorimetry, and differential scanning calorimetry (DSC). The results of these studies indicate that binding of nucleotides, particularly the GSAd adenylate analogue, are accompanied by significant conformation transitions.

MATERIALS AND METHODS

Materials. Adenosine 5′-triphosphate (ATP), 5′-adenylyl-imidodiphosphate (AMPPNP), adenylylmethylenediphosphonate (AMPPCP), α,β-methyleneadenosine 5′-diphosphate (AMPCPP), adenosine 5′-monophosphate (AMP), glycine, thrombin, Arg-C, and chymotrypsin were from Sigma. Glycine sulfamoyl adenosine (GSAd) was from RNA-Tec (Leuven, Belgium). Standard solutions of HCl and NaOH for calibration of the isothermal titration calorimeter were from Aldrich Chemical Co., St. Louis, MO. *B. mori g*lycyl-tRNA synthetase expressed in *E. coli* was purified as described earlier (*44*) and stored as concentrated solutions at 12−15 mg mL^{-1} at −80 °C.

Isothermal Titration Calorimetry. Titrations were performed in a titration calorimeter (Calorimetric Sciences Corp., Spanish Fork, UT) by making 25−30 injections of 2.5 μL of ligand into solutions of enzyme (1.2−1.25 mL) with a stir rate of 75 rpm and 300 s between injections. Titrations of ligand into buffer without enzyme were performed to determine the heats of dilution. After heats of dilution had been subtracted, differential heats of binding were analyzed using fits of single- and double-binding site models to extract the binding constant (K), the enthalpy (ΔH), and the binding stoichiometry (n) (*46*, *47*). Entropy (ΔS) was calculated from $\Delta G = \Delta H - T\Delta S$. Due to dilution of the first injection, it was not used for fitting. The instrument was calibrated by titration of 3 μL of a standard solution of 0.1036 M HCl into 1.0 mL of 0.0995 M NaOH at each temperature employed. Enzyme samples (200−300 μL at 12−15 mg mL^{-1}) were prepared for titrations by chromatography at room temperature on columns (5 mL) of Sephadex G50 superfine packed in a 5 mL disposable plastic pipet; buffer solutions contained buffer (as indicated), 5 mM $MgCl_2$, 0.5 mM dithiothreitol (DTT), and 50 mM KCl. Sephadex G50 chromatography was employed to exchange the solvent because dialysis resulted in significant inactivation of the enzyme. When phosphate buffer was employed, its concentration was 10 mM; the free phosphate under these conditions was 6.6 mM, and free Mg^{2+} was 1.6 mM. HEPES, MOPS, and Tris buffers were employed at 20 mM. Cacodylate buffers could not be employed due to reaction with protein thiols, which resulted in enzyme inactivation. Values for the ionization enthalpy of the buffers were taken from Fukada and Takahashi (*48*). After exchange of the buffer by Sephadex G50 chromatography, enzyme samples were degassed and centrifuged briefly (10 min) in a microcentrifuge. Enzyme concentration was determined spectrophotometrically ($\epsilon_{1\%,280nm} = 9.1$, $\epsilon_{M,280nm} = 7 \times 10^4$ for the subunit) (*37*, *44*). Protein concentrations employed in experiments ranged from 30 to 45 μM. Ligand solutions were prepared in the same buffer as enzyme; $MgCl_2$ was added such that the nucleotide existed as the 1:1 nucleotide−metal complex, and the free metal ion concentration was 5 mM except as noted for phosphate buffer. Concentrations of adenine nucleotide solutions were determined spectrophotometrically ($\epsilon_{M,259nm} = 15.4 \times 10^3$).

Differential Scanning Calorimetry. DSC experiments were performed using an N-DSCII differential scanning calorimeter (Calorimetric Sciences) using version 2 of the manufacturer's software for data acquisition and instrument control. Samples were prepared by chromatography on Sephadex G50 as described for isothermal titration calorimetry (ITC) experiments using 20 mM HEPES−KOH (pH 7.2), 5 mM $MgCl_2$, 0.5 mM DTT, and 50 mM KCl. Experiments were performed at 3 atm using a scan rate of 1 °C min^{-1}. Samples were scanned twice from 20 to 100 °C. Baselines were collected on the solvent and subtracted from the scans of protein samples. Unfolding of the protein was irreversible and accompanied by precipitation; accordingly, we could not obtain ΔC_p or ΔH for unfolding.

Enzyme Assays. Assays to determine values for Michaelis constants and inhibition constants were performed as described earlier (*44*). Assays were performed at five concentrations of ATP (0.005−0.05 mM) at four concentrations of glycine (0.1−1.0 mM) for determination of K_{ATP}; three concentrations of the nucleotide inhibitors were used for the determination of K_i.

Protease Digestion of Glycyl-tRNA Synthetase. Glycyl-tRNA synthetase (0.2 mg mL^{-1}) was incubated with proteases in reaction mixtures (15 μL) containing 20 mM HEPES−KOH (pH 7.5), 5 mM $MgCl_2$, 0.5 mM DTT, and 50 mM KCl. The proteases employed and their concentrations were as follows: thrombin, 50 units mL^{-1}; Arg-C, 10 μg mL^{-1}; and chymotrypsin, 2.5−10 μg mL^{-1}. Samples were incubated on ice, and aliquots were withdrawn at 24, 48, and 72 h and treated with SDS and mercaptoethanol for SDS gel electrophoresis (*49*) on 10% polyacrylamide gels.

[1] Abbreviations: DTT, dithiothreitol; GSAd, glycine sulfamoyl adenosine; SAS, solvent accessible surface area; ITC, isothermal titration calorimetry; DSC, differential scanning calorimetry.

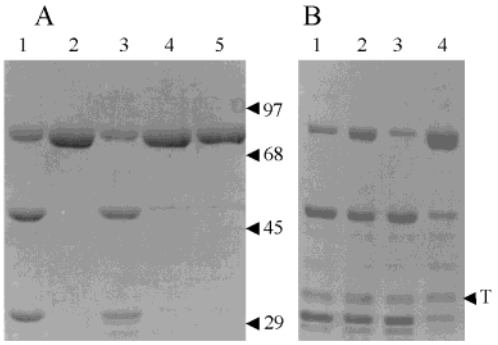

FIGURE 1: Proteolysis of glycyl-tRNA synthetase in the absence and presence of ligands: (A) (lane 1) enzyme digested with Arg-C, (lane 2) enzyme digested with Arg-C in the presence of 1 mM ATP, (lane 3) enzyme digested with thrombin, (lane 4) enzyme with thrombin in the presence of 1 mM ATP, (lane 5) enzyme incubated without protease; (B) (lane 1) enzyme digested with thrombin, (lane 2) enzyme digested with thrombin in the presence of 0.1 mM ATP, (lane 3) enzyme digested with thrombin in the presence of 1 mM glycine, (lane 4) enzyme digested with thrombin in the presence of 0.1 mM ATP and 1 mM glycine. The positions of molecular weight markers are indicated at the right of panel A. "T" at the right of panel B indicates the position of thrombin. Samples were applied to a 10% acrylamide SDS gel. Conditions of digestion are described under Materials and Methods.

Analysis of Glycyl-tRNA Synthetase by Gel Filtration. The oligomeric state of glycyl-tRNA synthetase was determined by analytical gel filtration on a 24 mL bed volume (0.5 cm × 30 cm) Superose 12 (Pharmacia) column using thyroglobulin (660 000 M_r), IgG (150 000 M_r), ovalbumin (45 000 M_r), and myoglobin (17 000 M_r) as standards. The column was equilibrated in 20 mM HEPES−KOH (pH 7.2), 5 mM $MgCl_2$, 50 mM KCl, and 0.5 mM DTT. Diluted samples of enzyme (400 μL) at concentrations ranging from 0.1 to 2 mg mL^{-1} were incubated at room temperature for 4−12 h and then applied to the column, which was run at room temperature. The column was eluted at 0.5 mL min^{-1}, and absorbance was monitored at 280 nm.

Collection of CD Spectra. CD spectra in the near-ultraviolet were collected using a Jasco J500 spectropolarimeter at 22 °C, employing a 1 mm path length cylindrical cell. Samples were prepared in 20 mM HEPES−KOH (pH 7.2), 5 mM $MgCl_2$, 50 mM KCl, and 0.5 mM DTT. Spectra were collected from 250 to 310 nm at 0.25 nm intervals, using a time constant of 64, at a scan rate of 1 nm min^{-1} and averaging three spectra. Protein concentration was 2.5 mg mL^{-1}.

RESULTS

Effect of Nucleotides on Proteolysis of Glycyl-tRNA Synthetase. We examined the effect of nucleotides on the digestion of native glycyl-tRNA synthetase by proteases as a simple method to detect potential conformational changes induced by nucleotide binding, an approach used with other aminoacyl-tRNA synthetases (*50*−*52*). As shown in Figure 1A, ATP rendered the enzyme resistant to digestion by thrombin and Arg-C. AMP, AMPPNP, AMPCPP, AMPPCP, and GSAd also protected the enzyme from digestion from thrombin and Arg-C, although at concentrations different from ATP without altering the pattern of fragments. Glycine alone had little effect, and *B. mori* $tRNA^{gly}$ had no effect on protease sensitivity. As shown in Figure 1B, ATP at low concentrations exerted a synergistic effect in combination with glycine, consistent with the formation of an enzyme-bound adenylate. Digestion of glycyl-tRNA synthetase with Arg-C generated a pattern similar to that obtained with thrombin, and we observed the same effects of nucleotides in mediating protection from proteolysis (results not shown). Digestion of glycyl-tRNA synthetase with chymotrypsin (not shown) generated a more complex pattern, but the presence of ATP afforded protection from digestion. The enzyme was quite resistant to digestion by trypsin. Because the effect of nucleotides could be nonspecific, we determined the concentration of nucleotide required to produce ~50% protection to determine if there was a correlation with the values for binding or inhibition constants. As shown in Table 1, the nucleotides that were the best inhibitors of enzyme activity were also the most effective at protecting the enzyme from proteolysis, although at higher concentrations than the K_m or K_i for the nucleotide. Glycyl-tRNA synthetase had no detectable enzymatic activity when AMPPNP or AMPPCP was substituted for ATP, and these compounds were competitive inhibitors with respect to ATP as were AMP and AMPCPP. These results are consistent with the nucleotides affording protection by binding at the nucleotide binding site, effectively ruling out trivial explanations, such as inhibition of the protease. That qualitatively similar results were obtained with different proteases further suggests that nucleotides may have a global effect on the structure of the protein.

Table 1: Kinetic Constants and IC_{50} Values for Thrombin Digestion for Glycyl-tRNA Synthetase

nucleotide	K_m or K_I, μM	IC_{50}, μM
ATP	13 ± 6	100
AMPPNP	20	100
AMPPCP	0.8	10
AMPCPP	60	600
AMP	80	800
GSAd	0.27 ± 0.08 (K_D, from ITC) 0.05 (K_I, from enzyme asays)	2

Characterization of the Binding of Nucleotides to Glycyl-tRNA Synthetase. We examined the energetics of nucleotide binding to glycyl-tRNA synthetase by isothermal titration calorimetry; examples of results from these experiments are shown in Figure 2 for ATP (panels A and B) and for GSAd (panels C and D). The data were analyzed by fitting with a single-site model, and the results are summarized in Figure 3 and Table 2; employing a two-site model did not result in a statistically significant improvemet in the fit to the data. Whereas the binding constant for AMPPNP was similar to that for ATP, those of AMPPCP and GSAd were 10−20-fold larger (Table 2). All of the nucleotides bound with a stoichiometry close to one per enzyme monomer. ATP, AMPPNP, and AMPPCP had similar values for ΔH with the differences in ΔG resulting from differences in $T\Delta S$, particularly for AMPPCP (Table 2 and Figure 3). The result is consistent with AMPPCP assuming a more constrained and presumably favorable conformation for binding. The binding constant for GSAd was similar to that for AMPPCP, but the value for ΔH was much larger and offset by a correspondingly large $T\Delta S$ term. The value for the K_I for GSAd (0.04 μM) determined from enzyme assays (Figure 4) was significantly lower than the dissociation constant

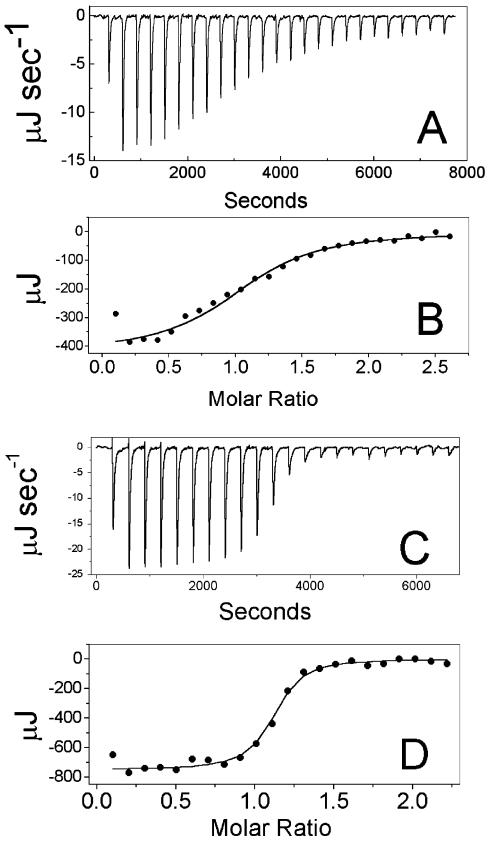

FIGURE 2: Isothermal titration calorimetry with glycyl-tRNA synthetase: (A) a solution of 2.34 mM MgATP was titrated into 1.25 mL of 46 μM glycyl-tRNA synthetase at 25.35 °C [ligand and enzyme were in 20 mM HEPES−KOH (pH 7.2), 5 mM $MgCl_2$, 0.5 mM DTT, and 50 mM NaCl]; (B) differential heats and fit to a one-site model; (C) a solution of 1.8 mM GSAd was titrated into 1.25 mL of a solution of 33.7 μM glycyl-tRNA synthetase with the other conditions the same as in panel A; (D) differential heats and fit to a one-site model.

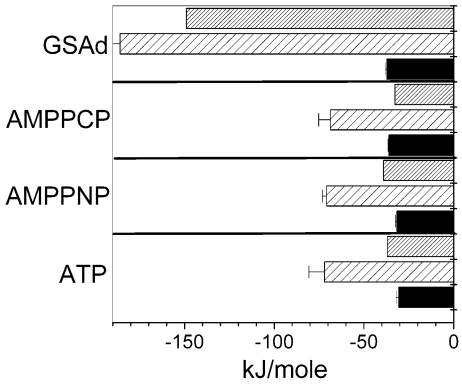

FIGURE 3: Summary of thermodynamic parameters at 25 °C for the binding of nucleotides to glycyl-tRNA synthetase. Solid bars are ΔG, sparsely hatched bars are ΔH, and densely hatched bars are $-T\Delta S$.

determined by ITC. As expected, GSAd was a competitive inhibitor with respect to ATP.

We examined the binding of the nucleotides by near-ultraviolet CD as shown for ATP in Figure 5. In the presence of ATP (panel A) the spectrum became more positive between 250 and 285 nm; the small signal for free ATP was subtracted from the spectrum for protein with ATP in panel A. The difference spectrum shown in panel B is almost the mirror image of the spectrum for free ATP, which was taken on a solution at a 10-fold higher concentration, compared to that used with the protein. Qualitatively and quantitatively similar results were obtained with AMPPNP and AMPPCP (not shown). On the basis of the binding constant for ATP obtained in the ITC experiments, >90% of the enzyme is bound to ATP. Free ATP exists as a mixture of the syn and anti configurations, with the equilibrium slightly favoring syn (*53*, *54*). Comparison of the difference spectrum in panel B to spectra of model compounds that exist exclusively in the syn or anti configuration indicates that ATP is bound to glycyl-tRNA synthetase in anti configuration as is the case for all class II aminoacyl-tRNA synthetases and the *T. thermophilus* glycyl-tRNA synthetase specifically (*28*, *31*). It is possible that there are changes in the aromatic region of the protein CD spectrum, but the CD of the bound nucleotide would likely mask these effects.

The most significant feature of the binding of the nucleotides was the large negative ΔH for the binding of GSAd. Included in this term are contributions from molecular interactions (*55*), coupled protonations (*47*), and any other coupled equilibria (*55*, *56*). The uptake or release of protons can occur when binding of ligand perturbs the pK_a of an ionizable group on the protein. To determine the extent to which coupled protonations contribute to ΔH_{obsd} for ATP and GSAd, we examined its dependence on the ionization enthalpy of different buffers employed for the titrations (phosphate, HEPES, MOPS, and Tris) as shown in Figure 6. Although there may be an uptake of one proton for the GSAd, this cannot account for the large enthalpy observed with GSAd. The value for ΔH for ATP showed little dependence on the ionization enthalpy of the buffer. It should be emphasized that this experiment does not include the heat of protonation arising from ionizable groups on the protein, only the heat coming from the buffer protonation or deprotonation. A systematic analysis of the pH dependence of binding might reveal the apparent pK_a, residue types, and their energetic contribution to the binding. Another possible source of the large negative ΔH is a change in the conformation of the ligand or a change in the oligomeric state of the protein. Because both conformers are well represented in the equilibrium between the syn and anti configurations of ATP, it is unlikely this equilibrium makes a significant energetic contribution to the value for ΔH_{obsd}. However, oligomerization of the protein coupled to binding could contribute significantly. Glycyl-tRNA synthetase is a dimer and does in fact dissociate to monomers (*32*, *37*), so binding of nucleotides coupled to a monomer−dimer equilibrium must be considered. To address this issue we have examined the oligomeric state of glycyl-tRNA synthetase by HPLC gel filtration under the solution conditions used for titration calorimetry over a range of concentration from 0.1 to 2 mg^{-1} mL^{-1}. The retention time always corresponded to that of dimer and was not changed by the presence of ATP in the elution buffer or by preincubation at room temperature for 4 h prior to application to the column. This result effectively rules out the possibility that the binding of nucleotides promotes dimerization, as was observed with the *S. cerevisiae* (*32*) glycyl-tRNA synthetase. The *B. mori* glycyl-tRNA synthetase dissociates to monomers under mild conditions in a concentration-dependent manner (*37*). It should be noted that these latter results were obtained under different solution conditions at 4 °C. The possibility that the

Table 2: Thermodynamic Parameters for Binding of ATP, AMPPNP, AMPPCP, and GSAd to Glycyl-tRNA Synthetase

nucleotide	ΔH, kJ mol^{-1}	ΔG, kJ mol^{-1}	$T\Delta S$, kJ K mol^{-1}	K, M^{-1}	n
ATP	-72 ± 8.6	-30.6 ± 1.4	-36.9 ± 4.2	$2.5 (\pm 1.4) \times 10^5$	1.01 ± 0.09
AMPPNP	-68 ± 6	-31.7 ± 0.7	-38.9 ± 2.6	$3.7 (0.95) \pm \times 10^5$	1.03 ± 0.16
AMPPCP	-70.7 ± 2.2	-36.3 ± 0.4	-31.7 ± 6	$2.17 (\pm 0.33) \times 10^6$	1.09 ± 0.03
GSAd	-187 ± 9.5	-37.4 ± 0.8	-149 ± 9.2	$3.7 (\pm 1.1) \times 10^6$	1.05 ± 0.025

[a] Values are the mean of three (AMPPNP, AMPPCP, and GSAd) or five (ATP) determinations. ΔG was calculated from $\Delta G = -RT \ln K$, where T is 298 K. The binding constants (K) and number of sites (n) per monomer were determined by titration calorimetry.

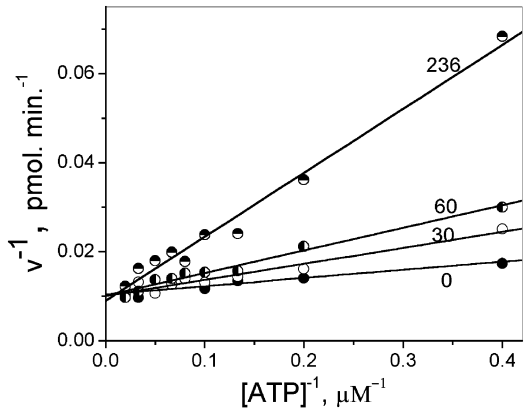

FIGURE 4: Inhibition of glycyl-tRNA synthetase by GSAd. Assays were performed in the absence or presence of the indicated concentrations of GSAd. The concentration of ATP ranged from 5 to 50 μM, and the concentration of glycine was 0.25 mM. Numbers on the plot indicate the concentrations (μM) of GS-Ad. Lines in the double-reciprocal plot are based on apparent values for V and K_{ATP} derived from nonlinear least-squares fits to a hyperbolic function ($v = V[ATP]/(K_{ATP} + [ATP])$.

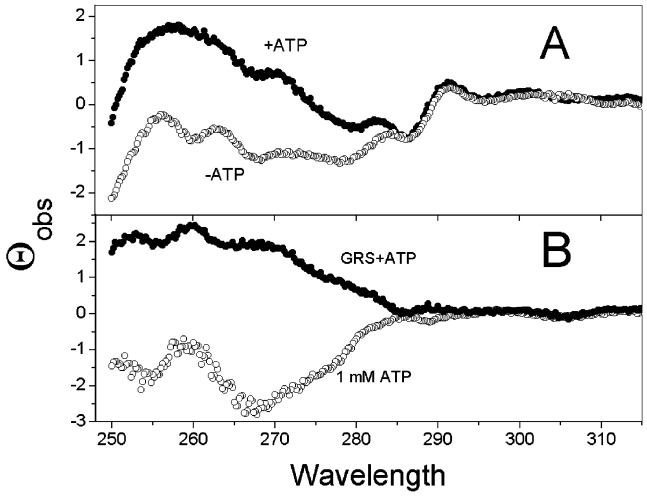

FIGURE 5: Near-UV CD spectra of glycyl-tRNA synthetase in the presence and absence of ATP: (A) CD spectra were recorded on a solution of glycyl-tRNA synthetase (2.4 mg mL^{-1}) in 20 mM HEPES−KOH (pH 7.2), 5 mM $MgCl_2$, 0.5 mM DTT, and 50 mM NaCl in the absence (solid symbols) or in the presence of 0.1 mM ATP (spectra were collected from 250 to 310 nm at 0.25 nm intervals, using a time constant of 64, at a scan rate of 1 nm per minute and averaging three spectra); (B) difference spectrum for glycyl-tRNA synthetase plus ATP and minus ATP (solid symbols) and 1 mM ATP alone (open symbols). Spectra were recorded in a 1 mM path cell.

binding of GSAd promotes the formation of monomers by binding preferentially to the monomer seems unlikely because the *T. thermophilus* glycyl-tRNA synthetase and many other dimeric class II enzymes have been crystallized as dimers with this type of ligand; in addition, the concentration of the monomeric species must be low because they were not detected in gel filtration experiments.

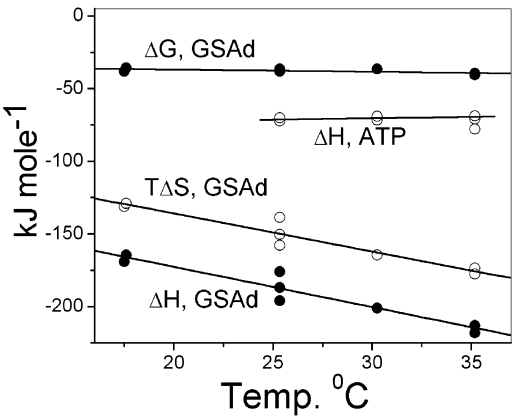

FIGURE 6: Dependence of ΔH_{obsd} on the ionization enthalpy of the buffer. Isothermal titration calorimetry was performed in buffers with different ionization enthalpies (phosphate, MOPS, HEPES, and Tris) at 25 °C. Open symbols show the results for ATP, and solid symbols show the results for GSAd.

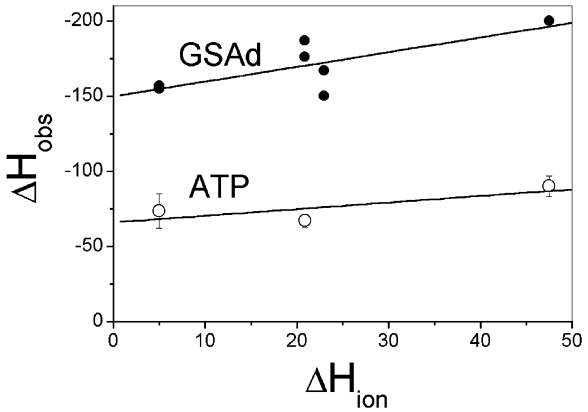

FIGURE 7: Dependence of ΔH_{obsd}, ΔG, and $T\Delta S$ for GSAd and ATP on temperature.

Another way to account for the large negative ΔH is through a conformational change in the protein coupled to binding (*57*, *58*). Such conformational changes can be reflected in a heat capacity change that accompanies binding, which in turn can be correlated with a change in solvent accessible surface area associated with the burial of nonpolar residues. To address this issue, we examined the dependence of ΔH of ATP and GSAd on temperature as shown in Figure 7. For GSAd there is little change in ΔG, but there is clear dependence of ΔH on temperature with a ΔC_p corresponding to -2.6 kJ K^{-1} mol^{-1}. The change in ΔH with temperature is accompanied by a compensating change in $T\Delta S$. The value for ΔH for ATP showed little dependence on temperature.

We examined the binding of nucleotides to glycyl-tRNA synthetase by DSC as shown in Figure 8. Thermodynamic

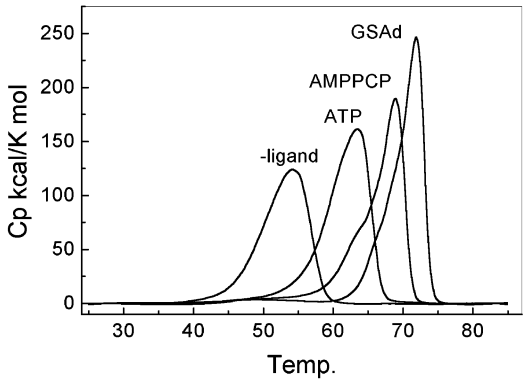

FIGURE 8: DSC on glycyl-tRNA synthetase in the absence and presence of ligands. The concentration of glycyl-tRNA synthetase was 2 mg mL^{-1}. The concentrations of nucleotides were ATP, 1 mM; AMPPCP, 1 mM; and GSAd, 0.5 mM.

parameters ΔC_p and ΔH for unfolding could not be extracted from these data because the transition temperature was scan rate dependent, the unfolding was irreversible, and the protein aggregated. Determining meaningful values for the thermodynamic parameters will require a detailed DSC analysis examining the effects of scan rate, pH, and ionic strength. However, there was a qualitative correlation with the binding constants obtained by ITC and the stabilization of the protein. AMPPCP and GSAd were the most effective at stabilizing the protein, whereas glycine alone afforded no stabilization nor did it alter stabilization by AMPPCP. Although GSAd and AMPPCP had similar binding constants, GSAd was more effective in stabilizing the protein. This difference between GSAd and AMPPCP in the DSC experiments is consistent with the difference in their binding enthalpies and the large negative heat capacity change associated with the binding of GSAd and indicates that the GSAd binds with greater affinity at its transition temperature than does AMPPCP at its transition temperature.

DISCUSSION

Binding of adenine nucleotides and a glycyl-adenylate analogue to glycyl-tRNA synthetase is an enthalpic driven process as revealed by isothermal titration calorimetry; stoichiometry for binding is approximately one per active site. Binding is also accompanied by significant stabilization of the protein to digestion by proteases and to thermally induced unfolding. GSAd binding has a large, negative enthalpy, which cannot be accounted for by protonation of the buffer or by binding being coupled to a monomer−dimer equilibrium. An example of a coupled equilibrium is seen in the binding of *E. coli* single-stranded DNA binding protein, where binding is coupled to unstacking of the bases of the single-stranded DNA (*59*). Other unrecognized equilibria are possible, but it is not immediately apparent what they might be because we have eliminated the most likely possibilities. One feature of the binding of GSAd that was not anticipated was its relatively small association constant (3.7×10^6 M^{-1}). Sulfamoyl adenylate and aminoalkyl adenylate analogues of the aminoacyl adenylates typically have K_I values in the low nanomolar range, consistent with moderately tight binding ligands. The relatively small binding constant suggests that GSAd has significant rotational freedom as reflected in the large $T\Delta S$ term. The adenylates of larger amino acids likely have more restricted conformations in solution. The binding of glycine to the enzyme, or perhaps it should noted as our failure to detect it, is likely a consequence of a relatively small binding constant; the Michaelis constant for the *B. mori* enzyme (0.35 mM, ref *44*) is at least 20 times that for the *T. thermophilus* enzyme (0.014 mM, ref *31*). If the value for the Michaelis constant reflects the binding constant, measuring binding constants by ITC for such a weakly binding ligand will be technically difficult due to the high protein concentration required.

The most unusual features of the binding of GSAd are the large binding enthalpy and the large negative heat capacity change (ΔC_p). Barring any effects from protonation or unrecognized equilibria mentioned above, such heat capacity changes are characteristic of significant changes in solvent accessible surface area that occurs as a result of burial of hydrophobic residues (*57*). Heat capacity changes have been related empirically to such phenomena by examining the solvent accessible surface area (SAS) of ligated and unligated acceptors for which ΔC_p values have been determined experimentally. Unfortunately, there are no X-ray structures for *B. mori* glycyl-tRNA synthetase, and the structures of the homologous *T. thermophilus* enzyme have some areas that are poorly ordered in the electron density map, effectively precluding a meaningful calculation of SAS. The *T. thermophilus* enzyme has the binding site for glycine and ATP largely preformed so that the structures of the glycyl−AMP and ethanolamine−ATP complexes differ little from that of the unligated enzyme (*26*). One would predict that a calculation of the value expected for ΔC_p upon binding of sulfamoyl adenosine to the *T. thermophilus* enzyme would not be as large as that obtained with the *B. mori* glycyl-tRNA synthetase. Two points need to be made on this issue. First, the *B. mori* and *T. thermophilus* enzymes are obviously different proteins, with the *B. mori* enzyme having additional structural elements; the active site of the eukaryotic enzyme may undergo significant rearrangements, due to these additional structural features, that do not occur with the prokaryotic enzyme. Second, the crystal structures of the free *T. thermophilus* glycyl-tRNA synthetase and its ligand complexes were, for obvious practical reasons, not obtained at the growth temperature of this organism. The structure of this enzyme would likely be considerably more dynamic at higher temperatures, a feature that could be evaluated by careful thermodynamic analysis of ligand binding. It may be that the inherently static nature of the protein−ligand complex and the free protein required to obtain crystals precludes detecting such a conformational transition. For comparison, thymidine binding and ATP binding to herpes simplex virus (HSV) type 1 thymidine kinase (*60*) are both highly exothermic (80 and 60 kJ mol^{-1}, respectively, at 25 °C). Binding of these ligands HSV TK is associated with negative heat capacity changes (−1.5 kJ mol^{-1} deg^{-1} for thymidine and −0.59 mol^{-1} deg^{-1} for ATP) that are 3 (thymidine) and 6 (ATP) times greater than values predicted from calculations based on the SAS of the ADP−dTMP ligated structure (*61*). Our findings suggest that binding of GSAd, and by extrapolation one would presume adenylate formation, is accompanied by significant conformational changes.

Perhaps the most interesting ligand, tRNA, is yet to be examined. Some significant questions are the following:

What are the energetics of tRNA binding, and how does the binding of cognate tRNA differ from that of noncognate tRNAs? How do mutations in identity elements alter the energetics of binding? Given the large enthalpy change that occurs upon adenylate analogue binding, are tRNA binding and recognition coupled to adenylate formation? The fact that the K_I in aminoacylation assays and the dissociation constant from ITC experiments are significantly different may indicate that the binding of one ligand alters the affinity of the enzyme for the other. Given the recent interest in the development of selective tRNA synthetase inhibitors that can be exploited as antimicrobial agents (*62*−*64*), understanding the thermodynamics of ligand interaction for this class of enzymes is particularly important in the design of selective drugs. Comparison of the energetics of binding of ligands to a prokaryotic tRNA synthetase and its eukaryotic counterpart could aid in the analysis of funtionalities on drugs that confer selectivity.

ACKNOWLEDGMENT

We thank Susan S. Dignam for critical comments on the manuscript.

REFERENCES

1. Ibba, M., and Soll, D. (2000) Aminoacyl-tRNA synthesis. *Annu. Rev. Biochem. 69*, 617−650.
2. Ivanov, K. A., Moor, N. A., and Lavrik, O. I. (2000) Non-canonical functions of aminoacyl-tRNA synthetases. *Biokhimiya (Moscow) 65*, 888−897.
3. Cusack, S. (1997) Aminoacyl-tRNA synthetases. *Curr. Opin. Struct. Biol. 7*, 881−889.
4. Ibba, M., and Soll, D. (2001) The renaissance of aminoacyl-tRNA synthesis. *EMBO Rep. 2*, 382−387.
5. Ibba, M., and Soll, D. (1999) Quality control mechanisms during translation. *Science 286*, 1893−1897.
6. Sankaranarayanan, R., and Moras, D. (2001) Fidelity of the translation of the genetic code. *Acta Biochim. Pol. 48*, 323−335.
7. Ribas de Pouplana, L., and Schimmel, P. (2001) Aminoacyl-tRNA synthetases: potential markers of genetic code development. *Trends Biochem. Sci. 26*, 591−596.
8. Hoagland, M. B., Keller, E. B., and Zamecnik, P. C. (1956) Enzymatic carboxyl activation of amino acids. *J. Biol. Chem. 218*, 345−358.
9. Hoagland, M. B., Zamecnik, P. C., and Stephenson, M. L. (1957) Intermediate reactions in protein biosynthesis. *Biochim. Biophys. Acta 24*, 215−216.
10. Hoagland, M. B., Stephenson, M. L., Scott, J. F., Hect, I. H., and Zamecnik, P. C. (1958) A soluble ribonucleic acid intermediate in protein synthesis. *J. Biol. Chem. 231*, 241−257.
11. Myers, C. A., Kuhla, B., Cusack, S., and Lambowitz, A. M. (2002) tRNA-like recognition of group I introns by a tyrosyl-tRNA synthetase, *Proc. Nat. Acad. Sci. U.S.A. 99*, 2630−2635.
12. Wallweber, G. J., Mohr, S., Rennard, R., Caprara, M. G., and Lambowitz, A. M. (1997) Characterization of *Neurospora* mitochondrial group I introns reveals different CYT-18 dependent and independent splicing strategies and an alternative 3′ splice site for an intron ORF. *RNA 3*, 114−131.
13. Herbert, C. J., Labouesse, M., Dujardin, G., and Slonimski, P. P. (1988) The NAM2 proteins from *S. cerevisiae* and *S. douglasii* are mitochondrial leucyl-tRNA synthetases, and are involved in mRNA splicing. *EMBO J. 7*, 473−483.
14. Wakasugi, K., and Schimmel, P. (1999) Two distinct cytokines released from a human aminoacyl-tRNA synthetase. *Science 284*, 147−151.
15. Shalak, V., Kaminska, M., Mitnacht-Kraus, R., Vandenabeele, P., Clauss, M., and Mirande, M. (2001) The EMAPII cytokine is released from the mammalian multisynthetase complex after cleavage of its p43/proEMAPII component. *J. Biol. Chem. 276*, 23769−23776.
16. Wakasugi, K., Slike, B. M., Hood, J., Ewalt, K. L., Cheresh, D. A., and Schimmel, P. (2002) Induction of angiogenesis by a fragment of human tyrosyl tRNA synthetase. *J. Biol. Chem. 277*, 20124−20126.
17. Wakasugi, K., Slike, B. M., Hood, J., Otani, A., Ewalt, K. L., Friedlander, M., Cheresh, D. A., and Schimmel, P. (2002) A human aminoacyl-tRNA synthetase as a regulator of angiogenesis. *Proc. Natl. Acad. Sci. U.S.A. 99*, 173−177.
18. Cusack, S. (1999) RNA-protein complexes. *Curr. Opin. Struct. Biol. 9*, 66−73.
19. Arnez, J. G., and Moras, D. (1997) Structural and functional considerations of the aminoacylation reaction. *Trends Biochem. Sci. 22*, 211−216.
20. Delagoutte, B., Keith, G., Moras, D., and Cavarelli, J. (2000) Crystallization and preliminary X-ray crystallographic analysis of yeast arginyl-tRNA synthetase-yeast $tRNA^{Arg}$ complexes. *Acta Crystallogr. Sect. D: Biol. Crystallogr. 56*, 492−494.
21. Cavarelli, J., Delagoutte, B., Eriani, G., Gangloff, J., and Moras, D. (1998) L-arginine recognition by yeast arginyl-tRNA synthetase. *EMBO J. 17*, 5438−5448.
22. Ruff, M., Krishnaswamy, S., Boeglin, M., Poterszman, A., Mitschler, A., Podjarny, A., Rees, B., Thierry, J. C., and Moras, D. (1991) Class II aminoacyl transfer RNA synthetases: crystal structure of yeast aspartyl-tRNA synthetase complexed with tRNA(Asp). *Science 252*, 1682−1689.
23. Dietrich, A., Giege, R., Comarmond, M. B., Thierry, J. C., and Moras, D. (1980) Crystallographic studies on the aspartyl-tRNA synthetase-$tRNA^{Asp}$ system from yeast. The crystalline aminoacyl-tRNA synthetase. *J. Mol. Biol. 138*, 129−135.
24. Arnez, J. G., Augustine, J. G., Moras, D., and Francklyn, C. S. (1997) The first step of aminoacylation at the atomic level in histidyl-tRNA synthetase. *Proc. Natl. Acad. Sci. U.S.A. 94*, 7144−7149.
25. Yaremchuk, A., Tukalo, M., Grotli, M., and Cusack, S. (2001) A succession of substrate induced conformational changes ensures the amino acid specificity of *Thermus thermophilus* prolyl-tRNA synthetase: comparison with histidyl-tRNA synthetase. *J. Mol. Biol. 309*, 989−1002.
26. Retailleau, P., Huang, X., Yin, Y., Hu, M., Weinreb, V., Vachette, P., Vonrhein, C., Bricogne, G., Roversi, P., Ilyin, V., and Carter, C. W. (2003) Interconversion of ATP binding and conformational free energies by tryptophanyl-tRNA synthetase: structures of ATP bound to open and closed, pre-transition-state conformation. *J. Mol. Biol. 325*, 39−63.
27. Koshland, D. E., Jr., Nemethy, G., and Filmer, D. (1966) Comparison of experimental binding data and theoretical models in proteins containing subunits. *Biochemistry 5*, 365−385.
28. Logan, D. T., Mazauric, M. H., Kern, D., and Moras, D. (1995) Crystal structure of glycyl-tRNA synthetase from *Thermus thermophilus*. *EMBO J. 14*, 4156−4167.
29. Fisher, E. (1894) *Ber. Dtsch. Chem. Ges. 27*, 2985−2893.
30. Freist, W., Logan, D. T., and Gauss, D. H. (1996) Glycyl-tRNA synthetase. *Biol. Chem. Hoppe Seyler 377*, 343−356.
31. Arnez, J. G., Dock-Bregeon, A. C., and Moras, D. (1999) Glycyl-tRNA synthetase uses a negatively charged pit for specific recognition and activation of glycine. *J. Mol. Biol. 286*, 1449−1459.
32. Kern, D., Giege, R., and Ebel, J. P. (1981) Glycyl-tRNA synthetase from baker's yeast. Interconversion between active and inactive forms of the enzyme. *Biochemistry 20*, 122−131.
33. Ge, Q., Trieu, E. P., and Targoff, I. N. (1994) Primary structure and functional expression of human glycyl-tRNA synthetase, an autoantigen in myositis. *J. Biol. Chem. 269*, 28790−28797.
34. Shiba, K., Schimmel, P., Motegi, H., and Noda, T. J. (1994) Human glycyl-tRNA synthetase. Wide divergence of primary structure from bacterial counterpart and species-specific aminoacylation. *J. Biol. Chem. 269*, 30049−30055.
35. Williams, J., Osvath, S., Khong, T. F., Pearse, M., and Power, D. (1995) Cloning, sequencing and bacterial expression of human glycine tRNA synthetase. *Nucleic Acids Res. 23*, 1307−1310.
36. Dignam, S. S., and Dignam, J. D. (1984) Glycyl- and alanyl-tRNA synthetases from *Bombyx mori*. Purification and properties. *J. Biol. Chem. 259*, 4043−4048.
37. Kawakami, M., and Nishio, K. (1985) Subunit structure and tRNA-binding properties of *Bombyx mori* glycyl-tRNA synthetase. *J. Biochem. 98*, 177−186.
38. Mazauric, M. H., Reinbolt, J., Lorber, B., Ebel, C., Keith, G., Giege, R., and Kern, D. (1996) An example of non-conservation of oligomeric structure in prokaryotic aminoacyl-tRNA syn-

thetases. Biochemical and structural properties of glycyl-tRNA synthetase from *Thermus thermophilus*. *Eur. J. Biochem. 241*, 814−826.
39. Cusack, S. (1993) Sequence, structure and evolutionary relationships between class 2 aminoacyl-tRNA synthetases: an update. *Biochimie 75*, 1077−1081.
40. Jeong, E.-J., Hwang, G.-S., Kim, K. H., Kim, M. J., Kim, S., Kim, K.-S. (2000) Structural analysis of multifunctional peptide motifs in human bifunctional tRNA synthetase: Identification of RNA-binding residues and functional implications for tandem repeats. *Biochemistry 39*, 15775−15782.
41. Cahuzac, B., Berthonneau, E., Birlirakis, N., Guittet, E., and Mirande, M. A. (2000) A recurrent RNA-binding domain is appended to eukaryotic aminoacyl-tRNA synthetases. *EMBO J. 19*, 445−452.
42. Seung, B. R., Lee, J. S., Jeong, E.-J., Kim, K.-S., Kim, Y. G., and Kim, S. (1998) A multifunctional repeated motif is present in human bifunctional tRNA synthetase. *J. Biol. Chem. 273*, 11267−11273.
43. Kaminska, M., Shalak, V., and Mirande, M. (2001) The appended C-domain of human methionyl-tRNA synthetase has a tRNA-sequestering function. *Biochemistry 40*, 14309−14316.
44. Wu, H., Nada, S., and Dignam, J. D. (1995) Analysis of truncated forms of *Bombyx mori* glycyl-tRNA synthetase: function of an N-terminal structure in RNA binding. *Biochemistry 34*, 16327−16336.
45. Schray, B., and Knippers, R. (1991) Binding of human glutaminyl-tRNA synthetase to a specific site of its mRNA. *Nucleic Acids Res. 19*, 5307−5312.
46. Freire, E., Mayorga, O. L., and Straume, M. (1990) Isothermal titration calorimetry. *Anal. Chem. 62*, 950A−959A.
47. Jelesarov, I., and Bosshard, H. R. (1999) Isothermal titration calorimetry and differential scanning calorimetry as complementary tools to investigate the energetics of biomolecular recognition. *J. Mol. Recog. 12*, 3−18.
48. Fukada, H., and Takahashi, K. (1998) Enthalpy and heat capacity changes for the proton dissociation of various buffer components in 0.1 M potassium chloride. *Proteins: Struct., Funct. Genet. 33*, 159−166.
49. Laemmli, U. K. (1970) Cleavage of structural proteins during the assembly of the head of bacteriophage T4. *Nature 227*, 680−685.
50. Pope, A. J., McVey, M., Fantom, K., and Moore, K. J. (1998) Effects of substrate and inhibitor binding on proteolysis of isoleucyl-tRNA synthetase from *Staphylococcus aureus*. *J. Biol. Chem. 273*, 31702−31706.
51. Kalogerakos, T. P., Dessen, G., Fayat, G., and Blanquet, S. (1980) Proteolytic cleavage of methionyl transfer ribonucleic acid synthetase from *Bacillus stearothermophilus*: effects on activity and structure. *Biochemistry 19*, 3712−3723.
52. Yanigasawa, T., Lee, J. T., Wu, H. C., and Kawakami, M. (1994) Relationship of protein structure of isoleucyl-tRNA synthetase with pseudomonic acid resistance of *Escherichia coli*; a proposed mode of action of pseudomonic acid as an inhibitor of isoleucyl-tRNA synthetase. *J. Biol. Chem. 39*, 24304−24309.
53. Miles, D. W., Townsend, L. B., Miles, D. L., and Eyring, H. (1979) Conformation of nucleosides: circular dichroism study on the syn-anti conformational equilibrium of 2-substituted benzimidazole nucleosides. *Proc. Natl. Acad. U.S.A. 76*, 553−556.
54. Miles, D. W., Robins, M. J., Robins, R. K., and Eyring, H. (1969) Circular dichroism of nucleoside derivatives. VI. The optically active bands of adenine nucleoside derivatives. *Proc. Natl. Acad. Sci. U.S.A. 62*, 22−29.
55. Sturtevant, J. (1977) Heat capacity and entropy changes in processes involving proteins. *Proc. Natl. Acad. Sci. U.S.A. 74*, 2236−2240.
56. Eftink, M. R., Anusiem, A. C., and Biltonen, R. L. (1983) Enthalpy−entropy compensation and heat capacity changes for protein ligand interactions: general thermodyanmic models and data for the binding of nucleotides to ribonuclease A. *Biochemistry 22*, 3884−3896.
57. Spolar, R. S., and Record, M. T. (1994) Coupling of local folding to site specific binding of proteins to DNA. *Science 263*, 777−784.
58. Ha, J. H., Spolar, R. S., and Record, M. T., Jr. (1989) Role of the hydrophobic effect in stability of site specific protein-DNA complexes. *J. Mol. Biol. 209*, 801−816.
59. Kozlov, A., and Lohman, T. M. (1999) Adenine base unstacking dominates the observed enthalpy and heat capacity changes for the *Escherichia coli* SSB tetramer binding to single-stranded oligoadenylates. *Biochemistry 38*, 7388−7397.
60. Perozzo, R., Jelesarov, I., Bosshard, H. R., Folkers, G., and Scapozza, L. (2000) Compulsory order of substrate binding to herpes simplex virus type thymidine kinase: a calorimetric study. *J. Biol. Chem. 275*, 16139−16145.
61. Wild, K., Bohner, T., Folkers, G., and Schulz, G. E. (1997) The structures of thymidine kinase from Herpes simplex virus type 1 in complex with substrates and a substrate analogue. *Protein Sci. 6*, 2097−2106.
62. Tao, J., and Schimmel, P. (2000) Inhibitors of aminoacyl-tRNA synthetases as novel anti-infectives. *Expert Opin. Invest. Drugs 9*, 1767−1775.
63. Brown, M. J., Mensah, L. M., Doyle, M. L., Broom, N. J., Osbourne, N., Forrest, A. K., Richardson, C. M., O'Hanlon, P. J., and Pope, A. J. (2000) Rational design of femtomolar inhibitors of isoleucyl tRNA synthetase from a binding model for pseudomonic acid-A. *Biochemistry 39*, 6003−6011.
64. Pope, A. J., Moore, K. J., McVey, M., Mensah, L., Benson, N., Osbourne, N., Broom, N., Brown, M. J., and O'Hanlon, P. (1998) Characterization of isoleucyl-tRNA synthetase from *Staphylococcus aureus*. II. Mechanism of inhibition by reaction intermediate and pseudomonic acid analogues studied using transient and steady-state kinetics. *J. Biol. Chem. 273*, 31691−31701.

BI030031H